

1 Cavitation growth phenomena in pure-sliding grease 2 EHD contacts

3 Takefumi Otsu^{1*}, Romeo Glovnea² and Joichi Sugimura³

4 ¹ Division of Mechatronics, Department of Innovative Engineering, Faculty of Science and Technology, Oita
5 University, 700 Dannoharu, Oita, 870-1192, Japan

6 ² Department of Engineering and Design, University of Sussex, United Kingdom

7 ³ International Institute for Carbon-Neutral Energy Research, Kyushu University, Japan

8 * Correspondence: ootsu-takehumi@oita-u.ac.jp

9 Received: date; Accepted: date; Published: date

10 **Abstract:** This article describes experimental and theoretical studies on the cavitation phenomena
11 in the grease lubrication film under pure sliding elastohydrodynamic contact. In-situ observation
12 tests using the optical interferometry technique were conducted, and the growth of cavitation was
13 captured using a high speed camera. The results showed that the cavity grew in two stages, which
14 was similar to the behaviour in the base oil, and that the cavity growth rate in the initial stage was
15 higher than that in the second stage. In the initial stage, the cavity growth time in the grease was
16 longer than that in the base oil, and the cavity length after the growth depended on the base oil
17 viscosity. It was also found in the test using diurea grease that small cavities were formed by the
18 lumps of thickener. The cavity growth in the initial stage was discussed by numerical simulation of
19 pressure distribution based on a simple rheological model.

20 **Keywords:** Cavitation; Elastohydrodynamic lubrication; Grease; Rheology; Gas
21

22 1. Introduction

23 Cavitation occurs in lubricated contact, and can be detrimental or beneficial to the performance
24 of machine elements¹). The phenomena related to cavitation include cavitation erosion, starvation,
25 breakdown of lubrication film in bearings, which are negative effects, but also reducing friction
26 coefficient and improving seal performance in seals and bearings, which are positive effects. **Recently,**
27 **the cavitation phenomena in the machine elements, such as journal bearing^{2,3}, seal⁴, pistonring-**
28 **cylinder liner^{5,6}, micro-textured surface^{7,8}, have been studied by the experimental observation and**
29 **the numerical simulation.**

30 One of the negative actions is the inlet starvation which leads to breakdown of lubrication film.
31 Nishikawa et al.⁹) have shown that short stroke length and/or large frequency, in reciprocated motion,
32 can lead to severe starvation of the contact, due to cavitation. The outlet cavitation also affects the
33 length of the meniscus at the inlet of contact in unidirectional rotating conditions^{10,11}). Severe
34 starvation is caused when the oil is not replenished into opened cavity area which is connected to the
35 atmospheric air, before the next contact. In grease lubrication, the amount of replenishment into the
36 cavity area is even smaller than that in the oil, because of the rheological properties of greases¹²). A
37 combined, experimental and theoretical analysis of cavitation and fretting wear of a grease lubricated,
38 a point elastohydrodynamic(EHD) contact has been carried out by Leonard et al¹³). Even at the low
39 velocities characteristic to fretting contacts, they have observed gaseous cavitation, whose length
40 extends with speed.

41 On the other hand, cavitation can reduce the friction coefficient in lubrication film due to lower
42 viscosity resistance force in the cavity region¹⁴⁻¹⁶). It has been reported by experimental approaches
43 that cavities formed in the micro pit on the ring surface¹⁶) and in the roughness on the rubber surface¹⁷)
44 is responsible for (deleted with) reducing the friction coefficient. The relationship between the sealing
45 mechanism and cavitation in lip or face seals is also known as positive actions. Anno and Walowit¹⁸)

46 reported that the load capacity on surfaces with micro-asperities is generated when cavitation occurs
47 on the outlet of asperity, because the pressure in the cavitation region is constant and then the positive
48 hydrodynamic pressure is greater than the negative one. This means that the lubrication performance
49 of the sealing surfaces with micro-texture is improved by the formation of cavitation^{17,19}. Cavitation
50 also affects the pressure-induced flow of lubricant, which implies that the leakage of lubricant from
51 the sealing system can be reduced by controlling the cavitation region⁴. From these facts it can be
52 concluded that, it is important to understand the behaviour of cavitation in various working
53 conditions for accomplishing safe and high performance machine components design.

54 Grease lubrication is widely used in many machine elements and especially rolling element
55 bearings and constant velocity joints, where they are preferred to oil lubrication. They hold important
56 advantages over oil lubricants such as lower lubricant losses, better corrosion protection, improved
57 sealing, easy to handle and the elimination of complex and costly oil supply system. Grease
58 lubrication also has disadvantages, such as poor heat convection which leads to thermal degradation
59 and limited free flow which leads to contact starvation. The complex nature of grease also makes it
60 difficult to predict the film thickness in lubricated contacts from its rheological properties²⁰. Extended
61 studies have been carried out in the past on various aspects of grease-lubricated EHD contacts
62 including the effect of thickener, the base oil and the working parameters²¹⁻²⁴. Kauzlarich and
63 Greenwood²⁵ applied the Herschel-Bulckley flow equation to grease lubricated EHD contacts,
64 carrying out a theoretical analysis of film. Yonggang and Jie²⁶ also started from the Herschel-Bulckley
65 model of flow, and introduced a shear rate and time-dependent structural parameter.

66 It is expected that the cavitation phenomenon in grease-lubricated films to be different from that
67 of oil lubrication films because of different rheology and flow properties. Cann et al.^{27,28} reported that
68 greases do not easily flow back onto the opened cavity area and the rolling track, thus, in the absence
69 of other mechanisms by which the lubricant is brought back in the inlet, severe starvation of the
70 contact occurs. Cavitation phenomena in grease lubrication have yet to be understood, especially the
71 difference between cavitation in the base oil and the grease. Therefore it is important to investigate
72 the cavitation phenomena in grease, for example the effect of rheological behaviour and of the
73 thickener, for the purpose of understanding their effect upon the lubrication performance.

74 One of the characteristics of cavitation is the growth phenomenon^{29,30}. The authors have studied
75 the cavity growth in oil lubricated point contacts in various environments^{31,32}. It has been reported
76 that the cavity grows in two stages; the initial stage in which the cavitation region shows rapid
77 growth and the second stage in which the growth rate is much lower than that in the first stage. The
78 growth in the initial stage is not affected by the amount of dissolved gas in the oil, and the growth
79 relates with the steep pressure drop generated at the outlet of the conjunction. The growth in the
80 second stage depends on the amount of dissolved gas. The cavity length in a gas environment with
81 higher gas solubility is longer, because the amount of released gas into the cavity is affected by the
82 dissolved gas in the oil. It has also been shown in the previous study that this cavity growth model
83 is applied in the high temperature and low pressure conditions^{33,34}.

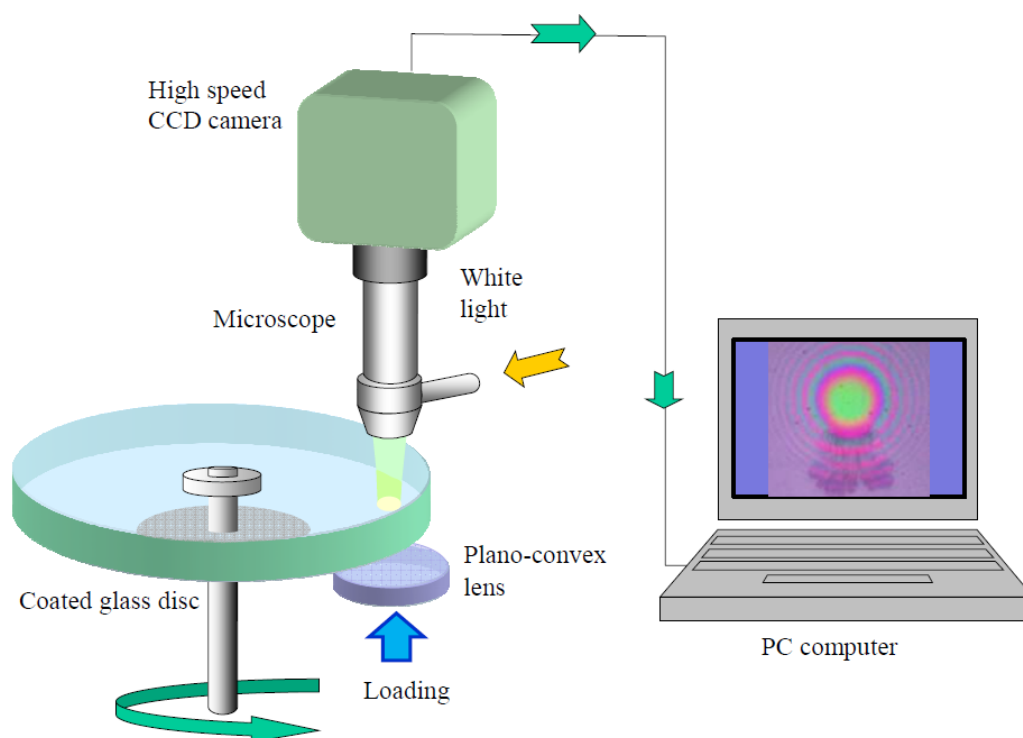
84 In this study, growth of the cavity in grease lubricated point contacts in pure sliding is
85 investigated. The difference of cavitation phenomena between the grease and the base oil, and the
86 effect of grease composition on the cavity growth are also discussed in this paper. In order to
87 understand the effect of the rheological properties of the greases on cavity growth, a simple numerical
88 analysis was conducted.

89 2. Experimental

90 2.1. Test Apparatus

91 Figure 1 shows a rig for measuring EHD film thickness by optical interferometry used in this
92 study. Greases and their base oils were tested in pure sliding, elastohydrodynamic point contact at a
93 room temperature of 295 K. A plano convex lens was pressed against a rotating disc by a lever, not
94 shown in the figure. The contact between the disc and the lens and the surrounding area were

95 observed through a custom built microscope, and interferometric images of the contact were
 96 recorded with a high speed CCD camera.



97
 98

Figure 1. Experimental set up.

99 The disc was made of optical glass and had a coating of a semi-reflective chromium layer on the
 100 working side. The diameter and thickness of the disc were 80 mm and 8 mm, respectively. The optical
 101 interferometry technique with the spacer layer imaging method (SLIM)³⁶ was employed to evaluate
 102 the lubricant film thickness, and an additional layer of silica was deposited on top of the chromium
 103 coating. The lens was also made out of optical glass and was coated with fully-reflective chromium
 104 layer. The radius of curvature of the lens was 10.38 mm.

105 Two series of tests were conducted in this study. The first series consisted of pure sliding tests
 106 at 20 mm/s constant speed, in which a load of 1 N (maximum Hertzian pressures of 0.14 GPa, and
 107 contact diameter of about 120 μm) was applied to the contact while the disc rotates at a constant speed
 108 of 20 mm/s. The second series of experiments were carried out under the accelerating conditions. The
 109 speed at the point of contact was increased from rest to 46.5 mm/s, in 17 milliseconds, which gave an
 110 acceleration of 2.7 m/s^2 . In these tests, the load employed was 7 N, which produced a maximum
 111 Hertzian pressure of 0.27 GPa, and a contact diameter of about 226 μm .

112 2.2. Greases

113 Five greases were studied in this work. The properties of these greases are shown in Table 1. The
 114 base oil of the greases was poly-alpha-olefin (PAO) with various viscosities. Thickeners were lithium
 115 stearate, lithium hydroxystearate and diurea. An amount of 0.2 ml of grease was uniformly spread
 116 onto the surface of the disc before each test. Grease or oil was not re-supplied into the contact during
 117 the tests.

118
 119
 120

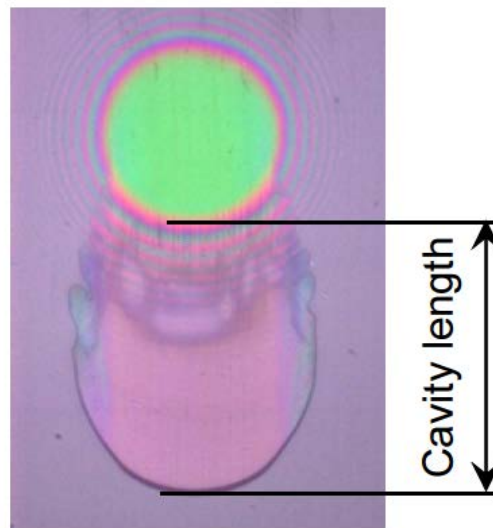
121

Table 1 Properties of greases.

No.	Thickener	Base oil viscosity @313, 373 K	Worked penetration (Consistency)
Grease 1	Lithium stearate, 12mass%	19, 4.1 [mm ² /s]	336
Grease 2	Lithium hydroxystearate, 12mass%	31, 5.8 [mm ² /s]	236
Grease 3	Lithium hydroxystearate, 12mass%	66, 10 [mm ² /s]	291
Grease 4	Lithium hydroxystearate, 12mass%	411, 41[mm ² /s]	386
Grease 5	Diurea, 13.4mass%	31, 5.8 [mm ² /s]	280

122 2.3. Definition of Cavity Length

123 Figure 2 shows an image of the contact and the surrounding area. The growth of cavity is
 124 described and analyzed in terms of cavity length which is defined as the length from the trailing edge
 125 of Hertzian contact to the trailing edge of the cavitation region, as shown in the figure.



126

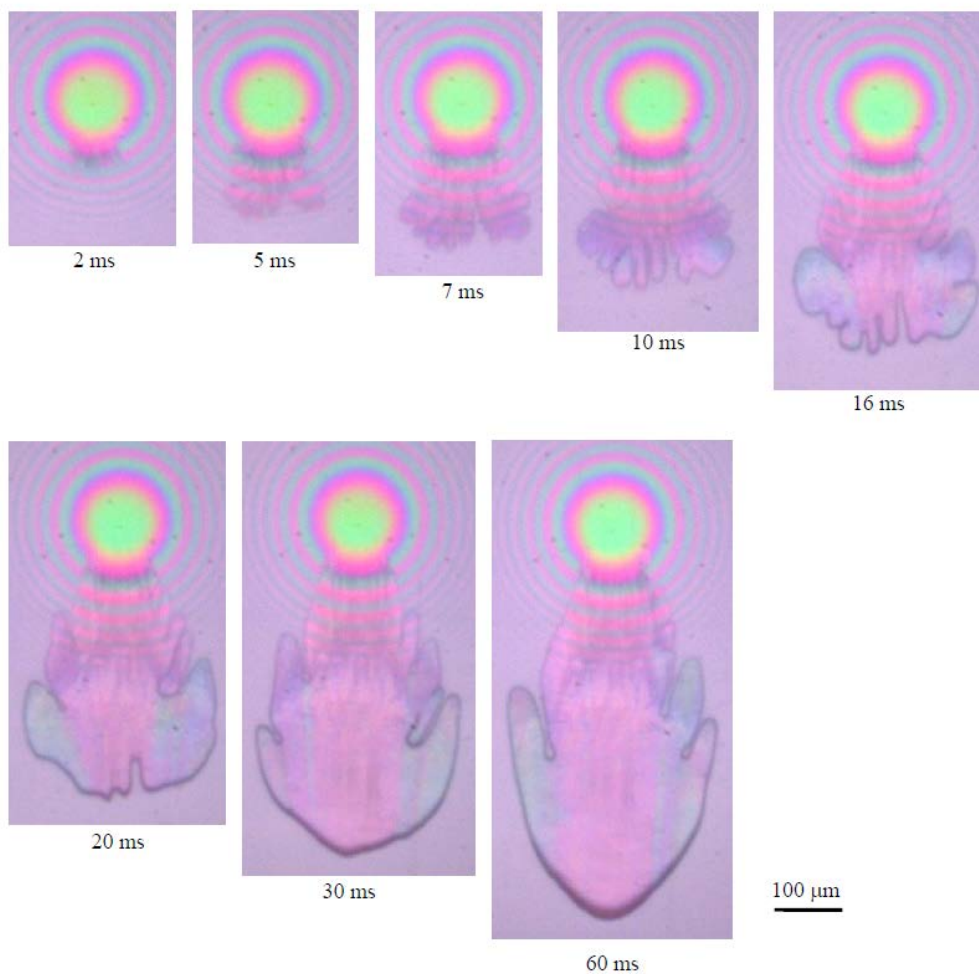
127

Figure 2. Definition of cavity length.

128 3. Results and Discussion

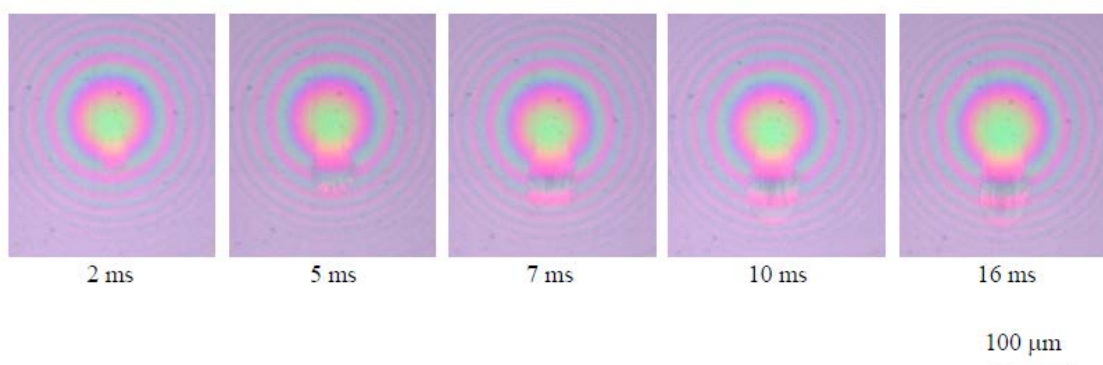
129 3.1. Cavity Growth: Grease Vs Base Oil

130 Figures 3 and 4 show interferometric images of the contact including the cavitation region for
 131 lithium stearate grease (Grease 1 shown in Table 1) and its base oil, from the start of the motion and
 132 up to 60 ms when the cavity length has stabilised. The tests were conducted under constant speed
 133 condition. Here, the central film thicknesses of the grease and the base oil were about 17 nm and 23
 134 nm, and the shear rate at the contact center were 1.2×10^6 and 0.9×10^6 s⁻¹, respectively.



135
136

Figure 3. Photographs of cavity in Grease 1 until 60 ms after the start.



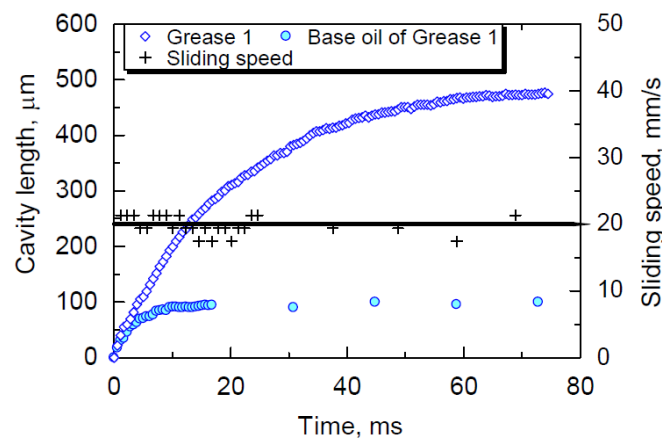
137
138

Figure 4. Photographs of cavity in base oil of Grease 1 until 16 ms after the start.

139 Figure 3 clearly illustrates that the cavitation region grows with time. In the image taken at 2 ms
140 the initiation of cavity is observed at the exit of contact. The cavity at times ranging between 2 and 20
141 ms shows the distinctive flower petal-like shape which Dowson et al.¹⁾ referred to as “fingers”. These
142 “petals” appear at the trailing edge of the cavity, and subsequently grow with time. With this type of
143 cavity shape, the gas dissolved in the lubricant is released into the cavity rapidly³²⁾. After about 30 ms
144 the cavity shape changes to a rather rounded shape.

145 As seen in Fig. 4 (deleted that) cavity growth for the base oil lubricated contact is similar to that
 146 of grease, that is the shape of cavity move after shape shows a petal-like shape, but this changes to
 147 monotonic rounded shape after only 10 ms.

148 Figure 5 shows the changes in cavity length with time. The cavity in the grease lubricated contact
 149 grows rapidly for the first approximately 30 ms and the growth slows down markedly after that. In
 150 the case of the base oil, on the other hand, the cavity length increases rapidly for the first 5 ms at
 151 which point the growth rate decreases and cavity length stabilizes at about 10 ms. The growth rates
 152 up to 3 ms for the grease and the base oil are 25 mm/s and 20 mm/s, respectively. Thus, in the initial
 153 stage of the cavity growth after the initiation, the growth rate is close to the sliding speed of the
 154 contact of 20 mm/s for both the grease and the base oil. After this initial stage, the cavity length
 155 increases further at different rates, for the two types of lubricants.



156
 157

Figure 5. Changes in cavity length from the start to 80 ms for Grease 1 and its base oil.

158 Figure 6 shows images of the cavitation region with lithium stearate grease (Grease 1) and its
 159 base oil at later stages from 0.1 s to 1 s. Figure 7 shows changes in cavity length up to one second after
 160 the start. Figures 6 and 7 demonstrate that the cavity grows gradually with time. Throughout the
 161 second stage, the growth rate of the grease is markedly higher than that in the base oil.

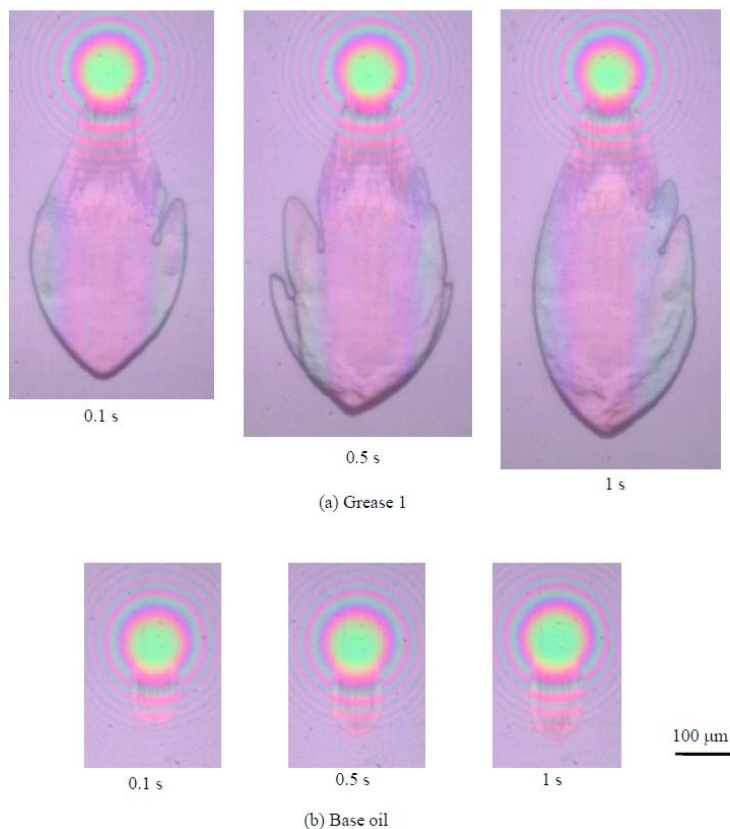


Figure 6. Photographs of cavity in Grease 1 and its base oil at 0.1, 0.5 and 1s.

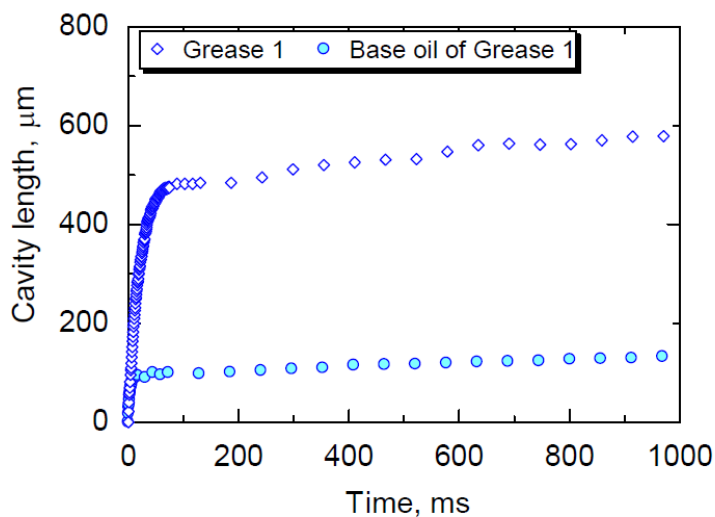


Figure 7. Changes in cavity length from the start to 1s for Grease 1 and its base oil.

162
163

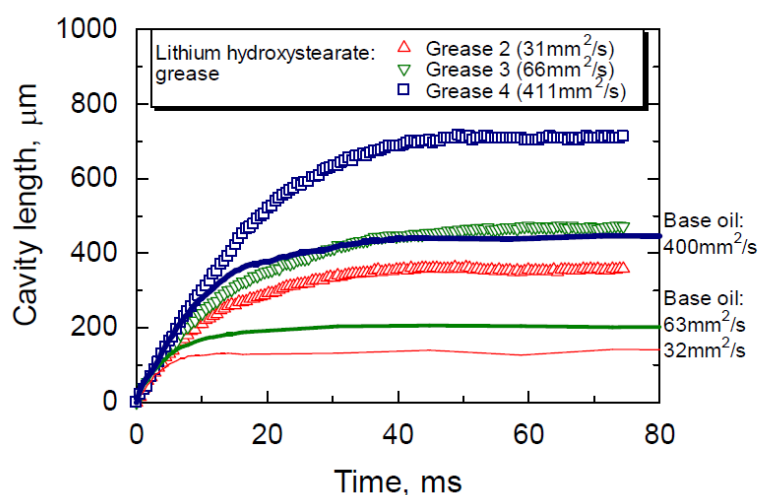
164
165

166 These results clearly show that the cavity in the grease film grows at two stages³². The initial
167 growth occurs after the initiation of the cavity and takes place at a fast rate approximately equal to
168 the sliding speed of the contact. The growth rates of the grease and the base oil are **similar** in this time
169 region, but the time for this initial growth is longer for the grease. In the second stage, the cavity
170 grows at a much slower rate, however the growth rate in the grease is still faster than that in the base
171 oil. The details of the mechanism in growth phenomenon will be discussed in the next chapter.

172 3.2. Effect of Base Oil Viscosity

173 In Fig.8, the changes in the cavity length with time is shown for three lithium hydroxystearate
 174 greases with different base oil viscosity, 31, 66, and 410 mm²/s at 313K (Grease 2, 3 and 4). The tests
 175 were conducted under constant speed condition. For comparison, changes of cavity length for the
 176 base oils are also shown.

177 The rate of cavity growth soon after the start is similar for greases with different base oil
 178 viscosity, but the duration in the initial stage is different; the time is longer for greases with higher
 179 base oil viscosity. At 60 ms after the initial growth, the cavity length is longer for greases with higher
 180 viscosity. Figure 8 also indicates that the cavity length at 60 ms for the base oil is shorter than that in
 181 the grease, while the growth rate in the initial stage is almost same for all the base oils and greases.
 182 Otsu³⁵⁾ previously found that the cavity region in the initial stage was affected by the negative
 183 pressure generated at the outlet of the contact, and the cavity length increased with the viscosity
 184 because the negative pressure depends on the viscosity. Stadler et al.³⁷⁾ also reported the relationship
 185 between the cavity length and the negative pressure. This behaviour is almost the same as that found
 186 for the grease in this study. This suggests that the growth time increases with base oil viscosity
 187 because the negative pressure region is larger for higher viscosity, and this holds also for the greases.



188

189

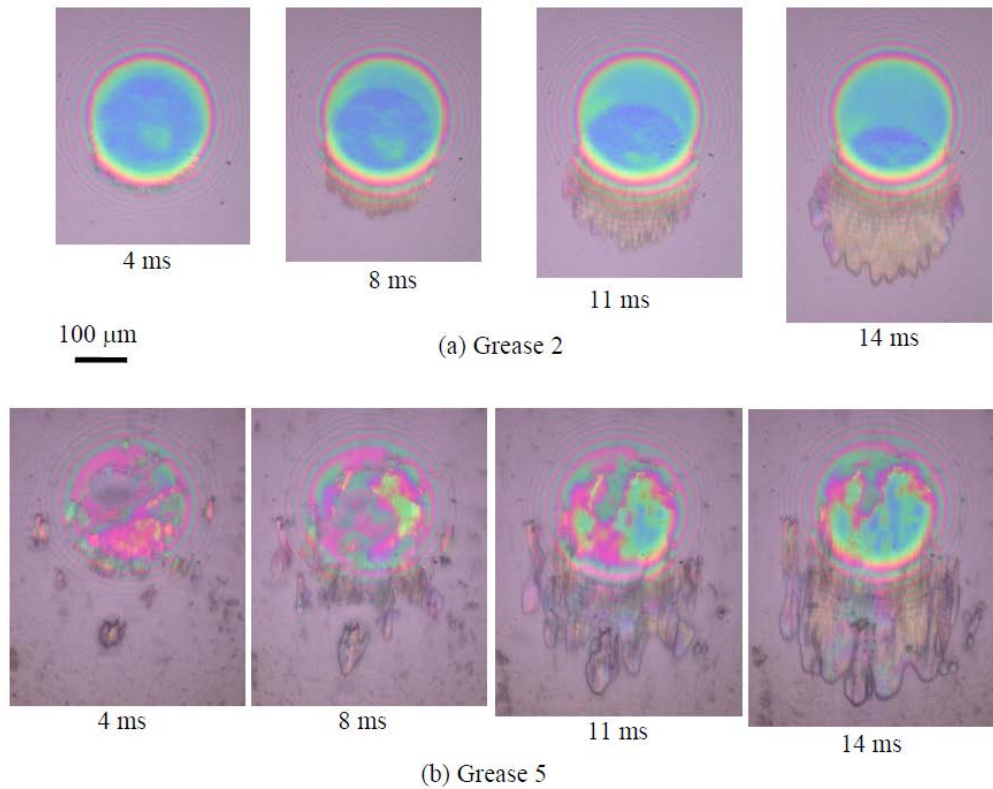
Figure 8. Effect of base oil viscosity on cavity growth for Grease 2, 3 and 4.

190 3.3. Effect of Thickener

191 Lithium hydroxystearate grease (Grease 2) and diurea grease (Grease 5) have been selected to
 192 study the effect of the thickener. Cavity growth under the accelerating condition was observed in this
 193 study.

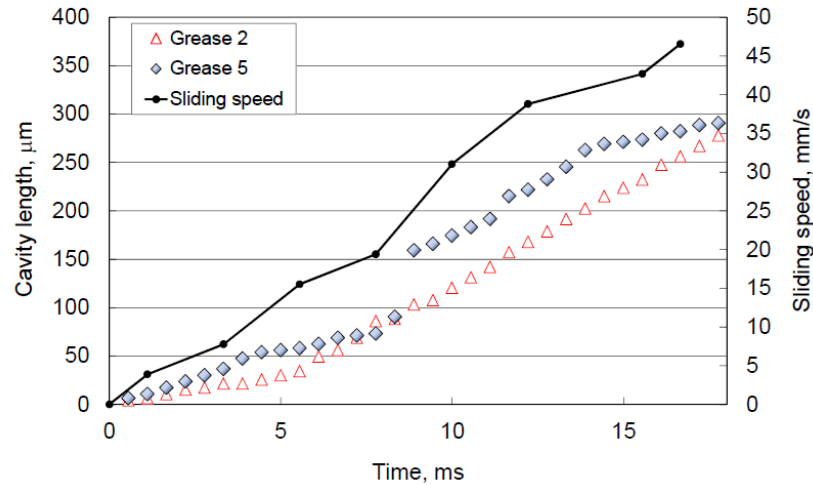
194 Figure 9 shows images of the cavity for the two greases. As it can be seen in these images, the
 195 cavity length changes from the start of the motion for both greases, but the shape of the cavitation
 196 region is different. For the lithium hydroxylstearate grease, the cavity shape is similar to that found
 197 for the base oil. This is obvious when comparing with the image taken at 7 ms shown in Fig. 3. In
 198 both cases, a number of petal-like projections appear at the trailing edge of the cavity. On the other
 199 hand, a number of cavities are formed by lumps of thickener soon after the start of the motion for
 200 diurea grease. It can be seen that pocket cavities are formed not only at the edge of contact, but also
 201 at other positions in the outlet region of the contact. Each of these individual cavities grow with time.
 202 At 14 ms these cavities have merged to form a single, larger cavity. Figure 10 shows the change of the
 203 cavity length with time. The variation of the sliding speed in these tests is also shown in Fig. 10. As it
 204 can be seen, (deleted that) the cavity length in diurea grease suddenly changes at 9 ms due to the
 205 merger of smaller cavities.

206



207
208

Figure 9. Cavity growth in Grease 2 and Grease 5.



209
210

Figure 10. Changes in cavity length during acceleration regime for Grease 2 and Grease 5.

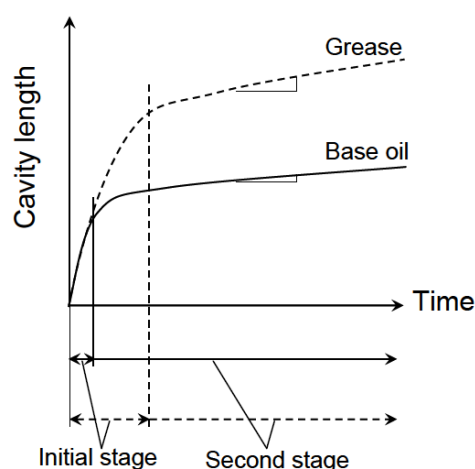
211 These results show that dispersion of the thickener in grease affects the formation of cavity.
212 Negative pressure is generated behind the thickener lumps, resulting in small cavities formed
213 partially at the outlet of contact. These small cavities may grow to a larger final cavity in some cases.

214 4. Cavity Growth Model in Grease Lubricated Contact

215 4.1. Two Stage of Cavity Growth

216 Figure 11 shows a schematic of the two-stage cavity growth revealed in this study. The results
217 in section 3.1 shows that initial growth is faster than the growth in the second stage, and that duration

218 of the initial stage in the grease is longer than that in the base oil. The time of initial growth is longer
 219 for the grease with higher base oil viscosity, as shown in section 3.2.



220
 221

Figure 11. Cavity growth in two stages.

222 A similar trend of the cavity growth was found for oil lubricants^{32,35}. Otsu et al.³² reported that,
 223 in the initial stage, cavity growth was related with the steep pressure drop at the exit of the EHD
 224 contact; dissolved gas was released rapidly because the pressure at outlet of contact drops to the
 225 saturation pressure of the gas. They also explained the mechanism in the initial stage by using a
 226 simple theoretical model. In the second stage, the cavity growth was caused mainly by the dissolved
 227 gas which was transferred to the cavity at cavity-lubricant boundary by the difference in the
 228 concentration, thus the cavity length increased gradually with time. These suggest that, in grease
 229 lubricated contact, the viscosity of grease and the amount of dissolved gas in the grease are the cause
 230 of the difference in the cavity growth between the grease and the base oil.

231 In the initial stage, the negative pressure distribution at the exit of the contact depends on the
 232 viscosity of the lubricant if the sliding speed and the shape of the gap are the same. As the viscosity
 233 of greases depend on shear rate, and should be greater than that of the oil, the pressure distribution
 234 should be different from that of the base oil. For greases with higher viscosity, the time of the initial
 235 stage of cavity growth should be longer because the pressure drop at the exit of contact is larger.
 236 Therefore, it would be worth extending the previous theoretical model to grease lubricated contacts
 237 by introducing the rheological properties of greases to see if these assumptions are correct. In
 238 addition, in case of diurea greases cavities are formed behind the thickener lumps, as shown in
 239 chapter 3.3. This reveals that, in the initial stage, the negative pressure distribution partially changes
 240 due to thickener lumps passing through the contact.

241 In the second stage, the previous study³⁵ showed that the cavity growth in greases was different
 242 for different surrounding gas and the length increased with increasing the gas solubility in the base
 243 oil. This implies that the cavity growth in greases occurred by the release of dissolved gas into cavity
 244 just as in the oil lubricated contact. In the present study, the experiments shown in section 3.1
 245 demonstrate that the cavity growth in the second stage is larger than that for the base oil. This
 246 suggests that the amount of dissolved gas in the grease is higher than that in the base oil. Another
 247 possible mechanisms for the larger cavity in the second stage in greases may be related with the
 248 replenishment capability of grease into cavity region. These two points will be addressed in future
 249 work.

250 4.2. Simple Numerical Analysis for Initial Stage of Cavity Growth

251 In order to understand the cavity growth in the initial stage, the simple theoretical analysis³² is
 252 extended here to grease lubricated contacts. In this analysis, a parametric study with model greases

253 is made in order to qualitatively understand the cavity growth with Grease 1 and its base oil shown
 254 in section 3.1. Pressure distribution in the divergent region of the conjunction is calculated by
 255 considering the viscosity of greases, and the relation between the negative pressure and cavity
 256 growth is discussed.

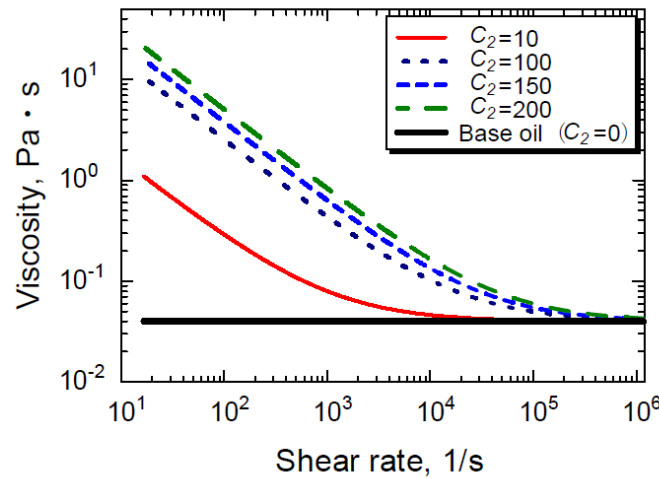
257 The shear dependence of the viscosity of greases is described here by the following simple
 258 equation:

$$\eta = C_1 + C_2 \dot{\gamma}^{m-1} \quad (1)$$

259 where η is viscosity, $\dot{\gamma}$ is shear rate, C_1 , C_2 and m are constants which determine the rheological
 260 behaviour of the fluid. In the case where C_1 and C_2 are not zero and m is equal to zero, Equation (1)
 261 corresponds to a Bingham plastic material. According to Sakurai and co-workers³⁸⁾, greases typically
 262 have C_1 equal to base oil viscosity and $m = 0.2$, while $m = 0.5$ for a softened grease. For oils, C_2 is zero,
 263 thus it is assumed that their viscosity does not depend on the shear rate. In this analysis, $0.04 \text{ Pa} \cdot \text{s}$
 264 is used for C_1 for the viscosity of the base oil of Grease 1 at 295K, and five values of C_2 , that is 0, 10,
 265 100, 150 and 200, are chosen. Index m was taken as 0.2, as suggested by Sakurai, thus the viscosity of
 266 grease used in the test shown in section 3.1, is given by:

$$\eta = C_1 + C_2 \dot{\gamma}^{m-1} = 0.04 + C_2 \dot{\gamma}^{-0.8} \quad (2)$$

267 Figure 12 illustrates the relationship between the viscosity and the shear rate given by Eq.(2).
 268 The viscosity of the grease decreases with the shear rate, and the value reaches to the base oil viscosity
 269 at high shear rate, of about at 10^6 s^{-1} which corresponds towards the value in lubrication film shown
 270 in the results in section 3.1.



271

272

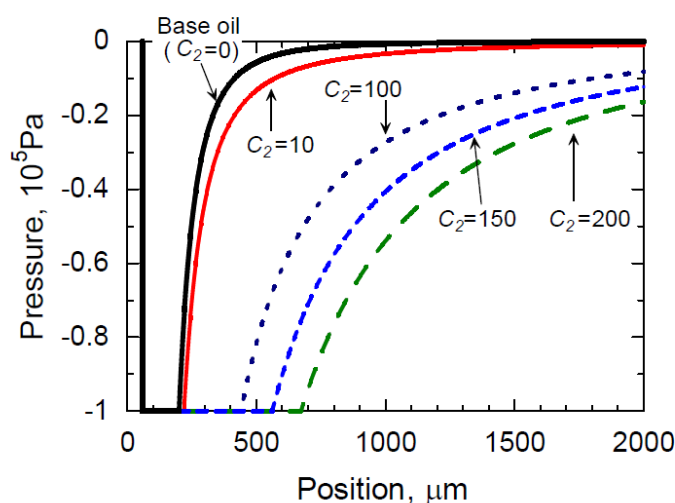
Figure 12. Relationship between viscosity and shear rate.

273 The pressure distribution at the outlet of the cavity region is evaluated by numerical calculation
 274 of the pressure given by Equation (3). Details of the derivation of this relationship are shown in the
 275 appendix.

$$p = 6C_1 U \left(\int_{x_i}^x \frac{1}{h^2} dx - h_m \int_{x_i}^x \frac{1}{h^3} dx \right) + 6C_2 U^{1+n} \left(\int_{x_i}^x \frac{1}{h^{2+n}} dx - h_m \int_{x_i}^x \frac{1}{h^{3+n}} dx \right) \quad (3)$$

276 In this equation, h is the separation between the solid surfaces, h_m is the separation corresponding
 277 to the local extreme value of the pressure and n has the value -0.8.

278 Figure 13 shows the pressure distribution at zero second for the base oil and three model greases
 279 with different C_2 . It clearly demonstrates that the region of absolute zero pressure, -0.1 MPa, is larger
 280 for the grease with higher C_2 . This is caused by higher viscosity.



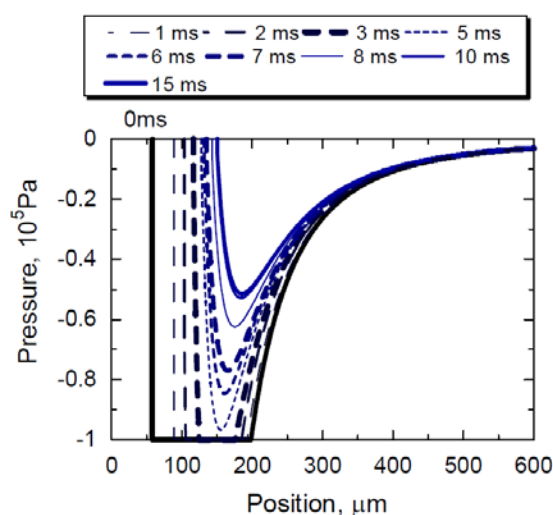
281

282

Figure 13. Effect of C_2 on negative pressure distribution.

283 Otsu et al. ^{32,35} reported that the cavity length after the initial growth is close to the length of -0.1
 284 MPa negative pressure region at zero second. This means that C_2 can be predicted by comparing the
 285 cavity length in the test and the calculated length of negative pressure region. Figure 13 shows that
 286 the length of -0.1 MPa region for C_2 of 150 is about 500 μm and this value is close to the cavity length
 287 after the initial growth of 450-470 μm , as shown in Fig.5. Thus, 150 is assumed to correspond to the
 288 value of C_2 for Grease 1.

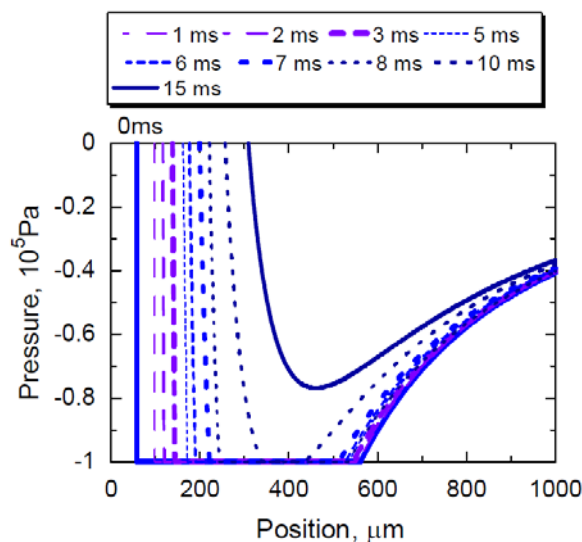
289 Figures 14, 15 and 16 show the variation with time of the calculated pressure distribution for the
 290 base oil and for the grease with $C_2=150$, respectively. The viscosity of the oil, sliding speed and film
 291 shape are the same with the values in the experiments, while the film thickness measured by the
 292 optical interferometry is used as h_{min} .



293

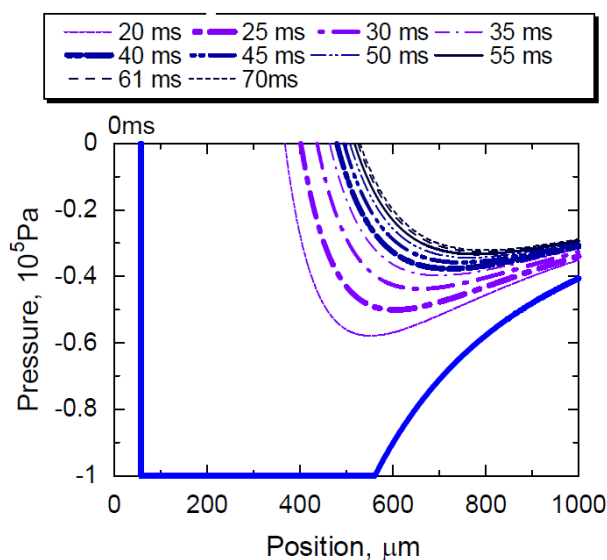
294

Figure 14. Changes in pressure distribution with time in base oil of Grease 1.



295
296

Figure 15. Changes in pressure distribution with time in grease with $C_2=150$.

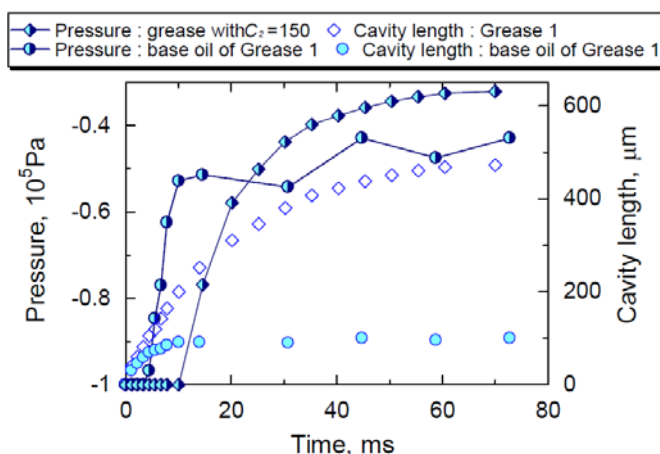


297
298

Figure 16. Changes in pressure distribution until 70 ms in grease with $C_2=150$.

299 In the pressure distribution, the -0.1 MPa region at zero s governs the initiation of cavity. Figures
300 14 and 15 clearly demonstrate that the length of the -0.1 MPa region is larger in the grease than in the
301 base oil. Also, the region of -0.1 MPa extends until 10 ms after the start for the grease and only until
302 3 ms for the oil, which is **similar** with the time for the rapid cavity growth shown in the experiments
303 in section 3.1. These figures also demonstrate that the pressure increases with time as the cavity grows
304 with time, and that the pressure distribution in the grease and the oil does not substantially change
305 after 55 ms and 10 ms, respectively.

306 Figure 17 shows the changes in the maximum negative pressure and the cavity length with time
307 for the base oil and the grease. In this figure, changes of the cavity length are for the test results of
308 Grease 1 and the base oil in section 3.1. All these figures demonstrate that rapid cavity growth occurs
309 when pressure drop is steeper and this happens for both the grease and oil. The cavity growth time
310 in the initial stage for the grease is longer because the steep pressure drop continues longer than for
311 the oil. This suggests that the difference in the cavity growth is caused by different rheological
312 properties. The shear rate dependence of the viscosity works to cause different growth behaviours.



313

314

Figure 17. Relation between minimum pressure and cavity growth for the grease and its base oil.

315 5. Conclusions

316 Cavitation in grease-lubricated EHD contacts has been studied with the optical interferometry
317 technique. The following conclusions are drawn from this study.

318 (1) Two stage cavity growths were observed in grease films, which is similar to those in the base
319 oil. The cavity growth rate in the initial stage is higher than that in the second stage, and the growth
320 time of the initial stage for the grease is longer than that for the base oil.

321 (2) The cavity length for greases is almost the same as that for their base oil up to 3 ms after the
322 start of sliding, but is longer than that in the base oil after 3 ms under the present test conditions.

323 (3) The growth time of the initial stage is longer for higher base oil viscosity. After the growth in
324 the initial stage, the cavity length for greases with higher base oil viscosity is longer.

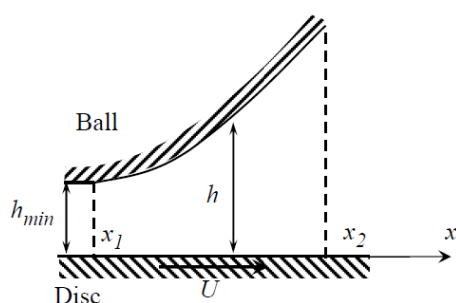
325 (4) In diurea grease, lumps of thickener cause the formation of smaller, individual cavities
326 immediately after the start.

327 (5) A theoretical analysis with a simple rheological model shows that the negative pressure
328 (below ambient) region in grease lubricated contacts is greater than that for the base oil, which
329 qualitatively agrees with the experimental results. The analysis suggests that the cavity growth in the
330 initial stage is related to steep pressure drop and its relaxation.

331 **Acknowledgements:** The authors express their gratitude to NSK Ltd. for supplying the greases.

332 Appendix

333 Consider the geometry of downstream of the contact between the ball and the disc at the exit
334 region, beyond the exit constriction, as illustrated in Figure A1²⁶).



$$x_1 = \text{Radius of Hertzian contact} + \text{Cavity length}$$

335

336

Figure A1. Geometry of the exit region of contact.

337 The separation between the surfaces h can be expressed by the relationship ³⁹⁾:

$$h = h_{\min} + \frac{a^2}{\pi R} \left(-2 - \frac{x^2}{a^2} \right) \cos^{-1} \frac{a}{x} + \left(\frac{x^2}{a^2} - 1 \right)^{0.5} \quad (\text{A1})$$

338 where a is the radius of the contact area and R the reduced radius of curvature of the surfaces.

339 It is obvious that the shear rate, defined as $\dot{\gamma} = U/h$ is not constant in this region, and according
340 to Equation (A1) the viscosity of the lubricant is assumed to vary with the position from the contact.

$$\eta = C_1 + C_2 \left(\frac{U}{h} \right)^n \quad (\text{A2})$$

341 The 2-D Reynolds equation is as follows:

$$\frac{dp}{dx} = 6\eta U \frac{h - h_m}{h^3} \quad (\text{A3})$$

342 where η is a function of h and implicitly of x .

343 By substituting (A1) and (A2) in (A3), separating the variables and integrating yield the
344 following expression for the pressure.

$$p = 6C_1 U \left(\int_{x_1}^x \frac{1}{h^2} dx - h_m \int_{x_1}^x \frac{1}{h^3} dx \right) + 6C_2 U^{1+n} \left(\int_{x_1}^x \frac{1}{h^{2+n}} dx - h_m \int_{x_1}^x \frac{1}{h^{3+n}} dx \right) + C_3 \quad (\text{A4})$$

345 where C_3 is a constant of integration. x_1 is $a + l_c$, where a is radius of the Hertzian contact area and l_c is
346 cavity length, if the axis x is taken from the center of the Hertzian contact, x_2 is the position of the end
347 of fully flood zone³²⁾.

348 As boundary conditions, the pressure at x_1 and x_2 is assumed to be zero. C_3 and h_m can be obtained
349 as follows:

$$C_3 = 0 \quad (\text{A5})$$

$$h_m = \frac{C_1 \int_{x_1}^{x_2} \frac{1}{h(x)^2} dx + C_2 U^n \int_{x_1}^{x_2} \frac{1}{h(x)^{2+n}} dx}{C_1 \int_{x_1}^{x_2} \frac{1}{h(x)^3} dx + C_2 U^n \int_{x_1}^{x_2} \frac{1}{h(x)^{3+n}} dx} \quad (\text{A6})$$

350 It follows that the pressure distribution is described by the following equation (A7).

$$p(x) = 6C_1 U \left(\int_{x_1}^x \frac{1}{h^2} dx - h_m \int_{x_1}^x \frac{1}{h^3} dx \right) + 6C_2 U^{1+n} \left(\int_{x_1}^x \frac{1}{h^{2+n}} dx - h_m \int_{x_1}^x \frac{1}{h^{3+n}} dx \right) \quad (\text{A7})$$

351 References

- 352 1. Dowson, D., Godet, M. and Tayler, C.M., "Cavitation and Related Phenomena in Lubrication", 1975,
353 Mechanical Engineering Publications Ltd.
- 354 2. Sakai, F., Ochiai, M. and Hashimoto, H., "CFD Analysis of Journal Bearing with Oil Supply Groove
355 Considering Two-Phase Flow", Proceedings of the 4th International Conference on Design Engineering and
356 Science, ICDES 2017, 2017, 131.
- 357 3. Otsu, T. and Nishida, K., "Growth of Cavitation in Journal Bearing and Effect of Cavitation on Behavior of
358 Bearing", Journal of Japanese Society of Tribologists, 2016, 61, 2, pp. 127-136 (in Japanese).
- 359 4. Tokunaga Y., Sugimura, J. and Yamamoto, Y., "Development and Performance Verification in Mechanical
360 Seals with Friction Reduction and Sealing Mechanism -Experimental Study-", Journal of Japanese Society

- 361 of Tribologists, 2015, 60, 5, pp. 332-341 (in Japanese).
- 362 5. Vasilakos, I., "Cavitation in the Cylinder-liner and Piston-ring Interaction in Internal Combustion Engines",
363 PhD thesis of City, University of Lindon, 2017.
- 364 6. Tang, T., Morris, N., Coupland, J. and Arevalo, L., "Cavitation Bubble Measurement in Tribological
365 Contacts Using Digital Holographic Microscopy", Tribology Letters, 2015, 58, 5, pp. 1-10.
- 366 7. Shen, C. and Khonsari, M.M., "On the Magnitude of Cavitation Pressure of Steady-State Lubrication",
367 Tribology Letters, 2013, 51, pp. 153-160.
- 368 8. Yagi, K., Sato, H. and Sugimura, J., "On the Magnitude of Load-Carrying Capacity of Textured Surfaces in
369 Hydrodynamic Lubrication", Tribology Online, 2015, 10, 3, pp. 232-245.
- 370 9. Nishikawa, H., Handa, K. and Kaneta, M., "Behaviour of EHL Films in Reciprocated Motion", JSME
371 International Journal., 1995, 38, 3, pp. 558-567.
- 372 10. Pemberton, J. and Cameron, A. A., "A Mechanism of Fluid Replenishment in Elastohydrodynamic Contacts",
373 Wear, 1976, 37, pp. 185-190.
- 374 11. Jackson, A. and Cameron, A., "An Interferometric Study of the EHL of Rough Surfaces", ASLE Transaction,
375 1976, 19, 1, pp. 50-60.
- 376 12. Cann, P.M.E., "Thin-film Grease Lubrication", Proceedings of Institution of Mechanical Engineers, 1999, 213,
377 Part J., pp. 405-416.
- 378 13. Leonard, B., Sadeghi, F. and Cipra, R., "Gaseous Cavitation and Wear in Lubricated Fretting Contacts",
379 Tribology Transaction, 2008, 51, 3, pp. 351-360.
- 380 14. Etsion, I., Halperin, G., Brizmer, V. and Kligerman, Y., "Experimental Investigation of Laser Surface
381 Textured Parallel Thrust Bearings", Tribology Letters, 2004, 17, 2, pp. 295-300.
- 382 15. Ryk, G., Kligerman, Y., Etsion, I. and Shinkarenko, A., "Experimental Investigation of Partial Laser Surface
383 Texturing for Piston-ring Friction Reduction", Tribology Transaction, 2005, 48, pp. 583-588.
- 384 16. Yagi, K., Takedomi, W., Tanaka, H. and Sugimura, J., "Improvement of Lubrication Performance by Micro
385 Pit Surfaces", Tribology Online, 2008, 3, 5, pp. 285-288.
- 386 17. Sato, Y., Seki, K., Sugimura, J. and Yamamoto, Y., "Experiments and Simple Modelling of Hydrodynamic
387 Lubrication in Radial Shaft Seals", Proceedings of the 17th international conference of fluid sealing, BHR
388 group, 2003, pp. 139-156.
- 389 18. Nau, B.S., "Film Cavitation Observation in Face Seals", Proceedings of the 4th International conference on
390 fluid sealing, BHRA, 1969, pp. 190-198.
- 391 19. Anno, J.N. and Walowit, J.A., "Microasperity Lubrication", Journal of lubrication Technology, 1968, pp.
392 351-355.
- 393 20. Sisko, A.W., "The flow of lubricating greases", Industrial and Engineering Chemistry, 1958, 50, 12, pp. 1789-
394 1792.
- 395 21. Dyson, A. and Wilson, A.R., "Film Thickness in Elastohydrodynamic Lubrication of Rollers by Greases",
396 Proceedings of Institution of Mechanical Engineers, 1970, 184, pp. 1-11.
- 397 22. Kaneta, M., Ogata, T., Takubo, Y. and Naka, M., "Effects of a Thickener Structure on Grease
398 Elastohydrodynamic Lubrication Films", Proceedings of Institution of Mechanical Engineers, 2000, 214,
399 Part J., pp. 327-336.
- 400 23. Couronné, I., Mazuyer, D., Vergne, P., Truong-Dinh, N. and Girodin, D., "Effects of Grease Composition
401 and Structure on Film Thickness in Rolling Contact", Tribology Transaction, 2003, 46, 1, pp. 31-36.
- 402 24. Eriksson, P., Wikstroëm, V. and Larsson, R., "Grease Passing Through an Elastohydrodynamic Contact
403 under Pure Rolling Conditions", Proceedings of Institution of Mechanical Engineers, 2000, 214, Part J., pp.

- 404 309-316.
- 405 25. Kauzlarich, J. and Greenwood, J.A., "Elastohydrodynamic Lubrication with Herschel-Bulckley Model
406 Greases", ASLE Transaction, 1972, 15, 4, pp. 269-277.
- 407 26. Yanggang, M. and Jie, Z., "A Rheological Model for Lithium Lubricating Grease", Tribology International,
408 1998, 31, 10, pp. 619-625.
- 409 27. Cann, P.M.E., "Starved Grease Lubrication of Rolling Contacts", Tribology Transaction, 1999, 42, pp. 867-
410 873.
- 411 28. Hurley, S., Cann, P.M. and Spikes, H.A., "Lubrication and Reflow Properties of Thermally Aged Greases",
412 Tribology Transaction., 2000, 43, 2, pp. 221-228.
- 413 29. Dowson, D., "Investigation of Cavitation in Lubricating Films Supporting Small Loads", Proceedings of
414 Conference on Lubrication and wear, 1957, pp. 93-99.
- 415 30. Archard, J.F. and Kirk, M.T., "Influence of Elastic Modulus on the Lubrication of Point Contacts",
416 Lubrication and Wear Convention, 1963, paper 15, pp. 181-189.
- 417 31. Otsu, T., Tanaka, H., Izumi, N. and Sugimura, J., "Effect of Surrounding Gas on Cavitation in EHL",
418 Tribology Online, 2009, 4, 2, pp. 50-54.
- 419 32. Otsu, T., Tanaka, H. and Sugimura, J., "Initiation and Growth of Gaseous Cavity in Concentrated Contact
420 in Various Surrounding Gas", Tribology International, 2012, 53, pp. 68-75.
- 421 33. Otsu, T., Tanaka, H. and Sugimura, J., "Effect of Temperature on Growth of Gaseous Cavitation in Point
422 Contact EHL", Journal of Japanese Society of Tribologists, 2014, 59, 10, pp. 648-656 (in Japanese).
- 423 34. Otsu, T., Tanaka, H. and Sugimura, J., "Effect of Surrounding Pressure on Cavity Growth in EHD contact",
424 Proceeding of International Tribology Conference Hiroshima 2011, 2011, E4-07.
- 425 35. Otsu, T., "Study on Cavitation in Elastohydrodynamic Lubrication", PhD thesis of Kyushu University, 2012
426 (in Japanese).
- 427 36. Cann, PM, Hutchinson, J. and Spikes H.A., "The Development of a Spacer Layer Imaging Method (SLIM)
428 for Mapping Elastohydrodynamic Contacts", Tribology Transaction, 1996, 39, pp. 915-921.
- 429 37. Stadler, K., Izumi, N., Morita, T., Sugimura, J. and Piccigallo, B., "Estimation of Cavity Length in EHL
430 Rolling Point Contact", ASME Transaction, Journal of Tribology, 2008, 130.
- 431 38. Sakurai, T., Hoshino, M. Tokashiki, M. and Fujita, M., "Grease for lubrication and synthetic lubricant", 1983,
432 Saiwai-syobou, pp. 80 (in Japanese).
- 433 39. Wedeven, L.D., Evens, D. and Cameron, A., "Optical analysis of ball bearing starvation", Transaction of
434 ASME, Journal of Lubrication Technology, 1971, 93, pp. 349-363.